Epstein-Barr virus nuclear protein EBNA3C directly induces expression of AID and somatic mutations in B cells

Jens S. Kalchschmidt,[1] Rachael Bashford-Rogers,[2] Kostas Paschos,[1] Adam C.T. Gillman,[1] Christine T. Styles,[1] Paul Kellam,[2] and Martin J. Allday[1]

[1]Molecular Virology, Department of Medicine, Imperial College London, London W2 1PG, England, UK
[2]Wellcome Trust Sanger Institute, Cambridge CB10 1SA, England, UK

Activation-induced cytidine deaminase (AID), the enzyme responsible for induction of sequence variation in immunoglobulins (Igs) during the process of somatic hypermutation (SHM) and also Ig class switching, can have a potent mutator phenotype in the development of lymphoma. Using various Epstein-Barr virus (EBV) recombinants, we provide definitive evidence that the viral nuclear protein EBNA3C is essential in EBV-infected primary B cells for the induction of AID mRNA and protein. Using lymphoblastoid cell lines (LCLs) established with EBV recombinants conditional for EBNA3C function, this was confirmed, and it was shown that transactivation of the AID gene (*AICDA*) is associated with EBNA3C binding to highly conserved regulatory elements located proximal to and upstream of the *AICDA* transcription start site. EBNA3C binding initiated epigenetic changes to chromatin at specific sites across the *AICDA* locus. Deep sequencing of cDNA corresponding to the IgH V-D-J region from the conditional LCL was used to formally show that SHM is activated by functional EBNA3C and induction of AID. These data, showing the direct targeting and induction of functional AID by EBNA3C, suggest a novel role for EBV in the etiology of B cell cancers, including endemic Burkitt lymphoma.

Activation-induced cytidine deaminase (AID) is an APOBEC-related enzyme that is essential in the affinity maturation of Ig heavy (IgH) and light (Ig-κ or Ig-λ, together referred to as IgL) chains during B cell differentiation (for review see Hwang et al. [2015]). Encounter between a mature B cell, its cognate antigen, and an antigen-specific T cell results in B cell activation and the expression of the transcriptional repressor BCL6 that is essential for the formation and maintenance of germinal centers (GCs) in secondary lymphoid tissue. BCL6-expressing B cells enter or initiate GCs and express high levels of AID that introduce somatic hypermutation (SHM) in the variable region of IgH and IgL through deamination of cytosine residues, which can be repaired by error-prone repair mechanisms to generate point mutants, some of which increase the affinity of membrane Igs for their cognate antigen. This is responsible for the process of affinity maturation. In addition, AID can cause DNA double-strand breaks that lead to Ig class switch recombination and the generation of B cells expressing IgG, IgA, or IgE (Hwang et al., 2015).

In addition to SHM and class switch recombination, AID is known to cause off-target lesions at non-Ig loci across the genome that can result in mutations and translocations in the development of cancer (for review see Robbiani and Nussenzweig [2013]). Many human B cell lymphomas are GC derived and express AID outside of the GC environment; these include Burkitt lymphoma (BL). BL are defined by characteristic chromosome translocation between the oncogene c-MYC and IgH or IgL, resulting in constitutive activation of c-MYC, but additional mutations of tumor suppressors, e.g., *TP53*, *CDKN2A*, or *BCL2L11* (BIM), are required for lymphomagenesis (for review see Schmitz et al. [2014]). The endemic form of BL (eBL) is etiologically associated with EBV and malaria (*Plasmodium falciparum*) infection (for review see Thorley-Lawson and Allday [2008]). Recently, it has been shown that *P. falciparum* can induce AID in human tonsillar B cells and that chronic malaria infection is associated with an increased GC transition of B cells (Torgbor et al., 2014). Furthermore, it was also shown that chronic malaria infection creates a GC environment favorable for the development of AID-dependent mature B cell lymphoma in a mouse model of *Plasmodium chabaudi* infection (Robbiani et al., 2015). However, until now, EBV was not regarded as actively driving eBL lymphomagenesis, but rather compensating for c-MYC–induced proliferative stress by repressing tumor suppressors and apoptosis-related factors, e.g., *CDKN2A* and *BCL2L11* (for review see Allday [2009] and Rowe et al. [2009]).

EBV is a human gamma-herpesvirus first discovered in eBL biopsies but also associated with other B cell lymphoma, e.g., Hodgkin lymphoma and immunoblastic lymphoma in

Correspondence to Martin J. Allday: m.allday@imperial.ac.uk

R. Bashford-Rogers's present address is Cambridge Institute for Medical Research, University of Cambridge, Cambridge CB2 0XY, England, UK.

Abbreviations used: AID, activation-induced cytidine deaminase; BL, Burkitt lymphoma; ChIP, chromatin immunoprecipitation; eBL, endemic form of BL; GC, germinal center; HT, 4-hydroxytamoxifen; LCL, lymphoblastoid cell line; RBPJ, recombination binding protein J; SHM, somatic hypermutation; TAP, tandem-affinity purification.

The Rockefeller University Press $30.00
J. Exp. Med. 2016 Vol. 213 No. 6 921–928
www.jem.org/cgi/doi/10.1084/jem.20160120

the immunosuppressed (for review see Young and Rickinson [2004]). However, most EBV infections occur early in life and have resulted in >90% of the global adult human population being asymptomatically and persistently infected. Infection of resting B cells with EBV results in activation and transformation into proliferating B blasts induced by the expression of EBV latency–associated genes producing six EBV nuclear antigens (EBNA1, 2, 3A, 3B, and 3C and leader protein), three latent membrane proteins (LMP1, 2A, and 2B), two small noncoding RNAs (EBER1 and 2), and microRNA transcripts from the BamHI A region (BARTs; Young and Rickinson, 2004; Skalsky and Cullen, 2015). The proliferating, infected B blasts, carrying extrachromosomal EBV episomes, then transit through a GC, and this is accompanied by gradual shutdown of viral gene expression and B cell differentiation, resulting in long-term persistence in the memory B cell population (for review see Thorley-Lawson [2015]). In vitro, infection of primary resting B cells with EBV creates continuously proliferating lymphoblastoid cell lines (LCLs) that again carry viral episomes constitutively expressing all of the latency-associated EBV genes.

In addition to the antiapoptotic role of EBV in B cell lymphomagenesis, various studies suggested that EBV infection could induce expression of AID (He et al., 2003; Tobollik et al., 2006; Epeldegui et al., 2007; Gil et al., 2007; Heath et al., 2012). However, none of these studies addressed the mechanism, definitively identified the EBV gene product responsible for the up-regulation, or ruled out preferential outgrowth of infected B cells with a preexisting high level of AID expression. Microarray analysis identified EBNA3C as a potentially important factor in the induction of AID (Skalska et al., 2013). EBNA3C is one of the viral oncoproteins that are essential for the in vitro transformation of B cells into LCLs and primarily acts as a transcriptional regulator of host gene expression (for review see Allday et al. [2015]). Here, we provide definitive evidence that EBNA3C is essential for the specific induction of AID in EBV-infected B cells and might therefore play a more active role in B cell lymphomagenesis than previously assumed.

RESULTS AND DISCUSSION

EBNA3C is necessary for the induction of AID after infection of primary resting B cells with EBV

We interrogated a sense target microarray (Exon 1.0 ST; Affymetrix) with cDNA from EBNA3C-conditional LCLs (3CHT) and identified EBNA3C as a potential viral factor necessary for the induction of AID because *AICDA* was the gene most highly up-regulated by EBNA3C (Skalska et al., 2013). To establish that AID is actually regulated by EBNA3C during viral infection, primary $CD19^+$ B cells were infected with previously constructed and characterized EBNA3C KO and revertant (Rev) EBV recombinants (Anderton et al., 2008). Infection with EBNA3C Rev virus resulted in a gradual induction of AID mRNA to high levels (>20-fold above resting B cells) over a period of ∼30 d (Fig. 1). However, this induction of AID was not observed after infection with EBNA3C KO virus; here, AID mRNA levels remained similar to those seen in the uninfected primary B cells. This identified EBNA3C as an essential factor for the induction of AID and also ruled out the possibility that EBV infection led to the preferential outgrowth of B cells with a preexisting high level of AID expression. Moreover, consistent with previous studies (Gil et al., 2007; Heath et al., 2012), BCL6 was well repressed by EBV, and this was independent of the presence or absence of functional EBNA3C over the same period (Fig. S1 A). This suggests that EBV transformation does not mimic the establishment of GC-like cells in other critical respects.

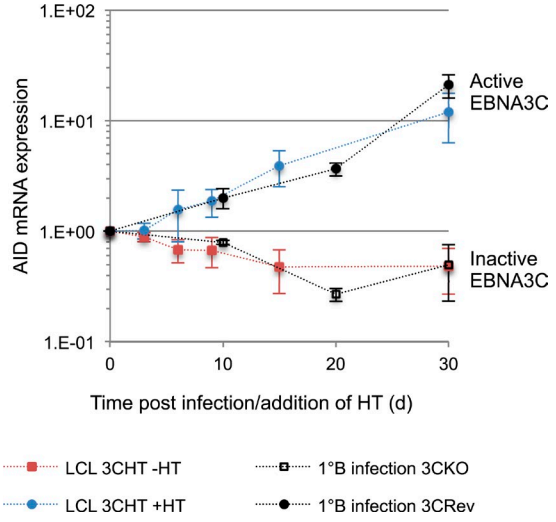

Figure 1. **EBNA3C induces AID expression after infection of primary B cells with EBV and in EBNA3C-conditional LCLs.** Primary B cells infected with EBNA3C KO (3CKO) or revertant (3CRev) recombinant EBV were cultured over a period of 30 d. EBNA3C-conditional LCLs (3CHT) were cultured over a period of 30 d in the absence (−HT) or presence (+HT) of HT. AID mRNA expression was normalized to *GAPDH* or *GNB2L1* and is shown relative to uninfected primary B cells or 3CHT cells on day 0. Results show the mean ± SD of three biological replicates. B cells from different donors were used for the infections. Please note that the day 30 time point of 3CKO-infected primary B cells shows the mean of two replicates.

Regulation of AID can be recapitulated in EBNA3C-conditional LCLs

Having established that EBNA3C is essential for the induction of AID after primary infection, we wanted to determine whether this was recapitulated in the 3CHT LCLs that carry EBV recombinants with conditional EBNA3C. In these cell lines, EBNA3C activity is conditional on the presence of 4-hydroxytamoxifen (HT), but proliferation of the cells does not decrease in its absence because of the homozygous deletion of $p16^{INK4A}$, a primary target of EBNA3C (Skalska et al., 2013). An LCL could therefore be established in the absence of functional EBNA3C or high levels of AID (3CHT A13). Activation of EBNA3C by the addition of HT to these cells (+HT) resulted in an increase of AID

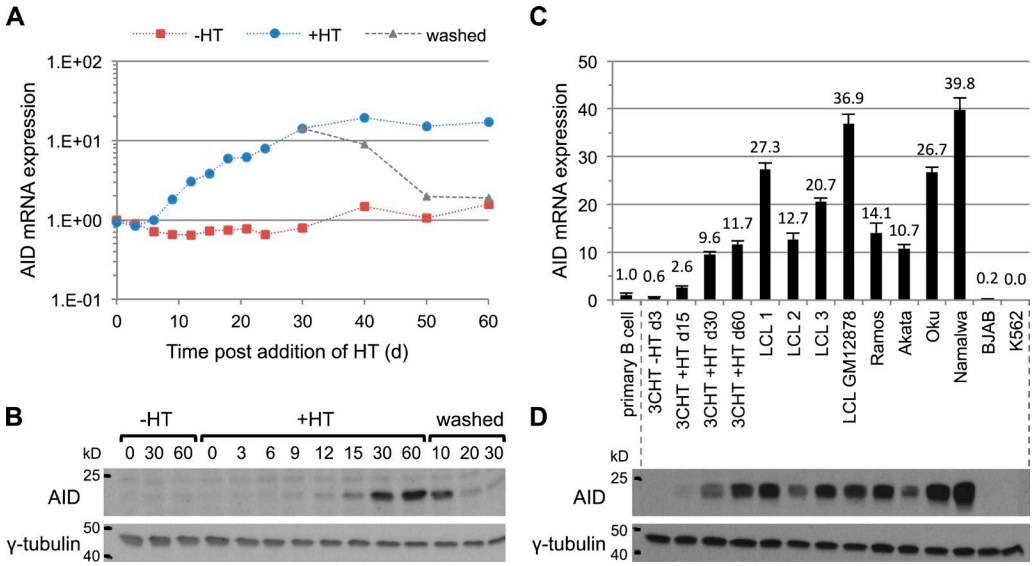

Figure 2. **Induction of AID mRNA and protein in EBNA3C-conditional LCLs and comparison across various cell lines.** (A) Time course using EBNA3C-conditional LCL 3CHT A13. Cells were grown over a period of 60 d in the absence of HT (−HT), in the presence of HT (+HT), or with HT removed after 30 d +HT (washed). Gene expression for AID was normalized to *GAPDH* and is shown relative to −HT on day 0. (B) Western blot showing AID and γ-tubulin protein expression in selected samples (numbers indicate time point) of the 3CHT A13 time course shown in A. (C) AID mRNA expression in 3CHT LCLs, three in-house B95.8 EBV–transformed LCLs (1, 2, and 3), LCL GM12878, Ramos (EBV-negative BL), EBV-positive BL (latency I Akata [not expressing EBNA3C], EBV W-promoter [Wp]–restricted Oku [expressing EBNA3C], and latency III Namalwa [expressing EBNA3C]), BJAB (EBV-negative B cell lymphoma), and K562 (EBV-negative erythromyeloblastoid leukemia) were normalized to GAPDH and are shown relative to primary B cells. Results show the mean ± SD of three technical replicates. (D) AID and γ-tubulin protein expression in samples shown in C. A and B show representative results of three biological replicates, and C and D show representative results of at least two biological replicates.

mRNA expression very similar in magnitude and timing to that seen after infection of primary B cells with EBNA3C Rev virus (Fig. 1). No increase in AID levels was observed when EBNA3C remained inactive (−HT), which displayed AID levels comparable with resting B cells or primary B cells infected with EBNA3C KO virus.

Fig. 2 (A and B) shows a representative 3CHT time course over a 60-d period. Maximal AID mRNA (Fig. 2 A) and protein (Fig. 2 B) expression levels were detected 30 d after activation of EBNA3C, which was fully reversible by inactivation of EBNA3C after withdrawal of HT. In the absence of functional EBNA3C, 3CHT cells expressed AID at levels similar to uninfected primary B cells, and when EBNA3C was switched on, AID levels were comparable with those in various BL cell lines and various LCLs independently established with B95.8 EBV (Figs. 2, C and D). Some LCLs expressed remarkably large amounts of AID mRNA and protein, and it is perhaps worth noting that GM12878, which was used as the tier 1 LCL in the Encyclopedia of DNA Elements (ENCODE), is one of them.

EBNA3C targets highly conserved regulatory elements to induce epigenetic changes for AID expression

Next, to determine whether induction of AID is a direct or indirect effect of EBNA3C expression, we analyzed chromatin immunoprecipitation (ChIP) coupled to sequencing (ChIP-Seq) performed on tandem-affinity purification (TAP)–tagged EBNA3C-expressing LCLs (unpublished data). This revealed EBNA3C occupancy at most (4/5) of the previously identified and highly conserved regulatory regions of the *AICDA* gene (Fig. 3 A). Region I contains the *AICDA* promoter, region II is located within the first intron, and region IV is located ∼17 kb upstream of the transcriptional start site (Zan and Casali, 2013). In addition, two more recently identified regions, V and VI, are situated ∼32 and ∼36 kb upstream of the transcriptional start site, respectively (Kieffer-Kwon et al., 2013). Most of these regions were initially identified in mouse B cells, but they are highly conserved in human B cells, and the whole locus has been called the AID/*AICDA* superenhancer (Fig. 3 A; Qian et al., 2014). Different levels of EBNA3C occupancy were observed at these regulatory elements in the following order of magnitude: VI > IV > II > V, which was confirmed by ChIP-qPCR (Fig. S2).

Therefore, it seemed that the induction of AID was a direct effect of EBNA3C binding to regulatory regions at the *AICDA* locus, which raised the question of how EBNA3C induced AID expression. EBNA3C is primarily known as a transcriptional coregulator, but it has been studied most frequently in gene repression (Allday et al., 2015). ChIP samples harvested during the 3CHT time course from cells expressing functional or nonfunctional EBNA3C were therefore analyzed for changes in activa-

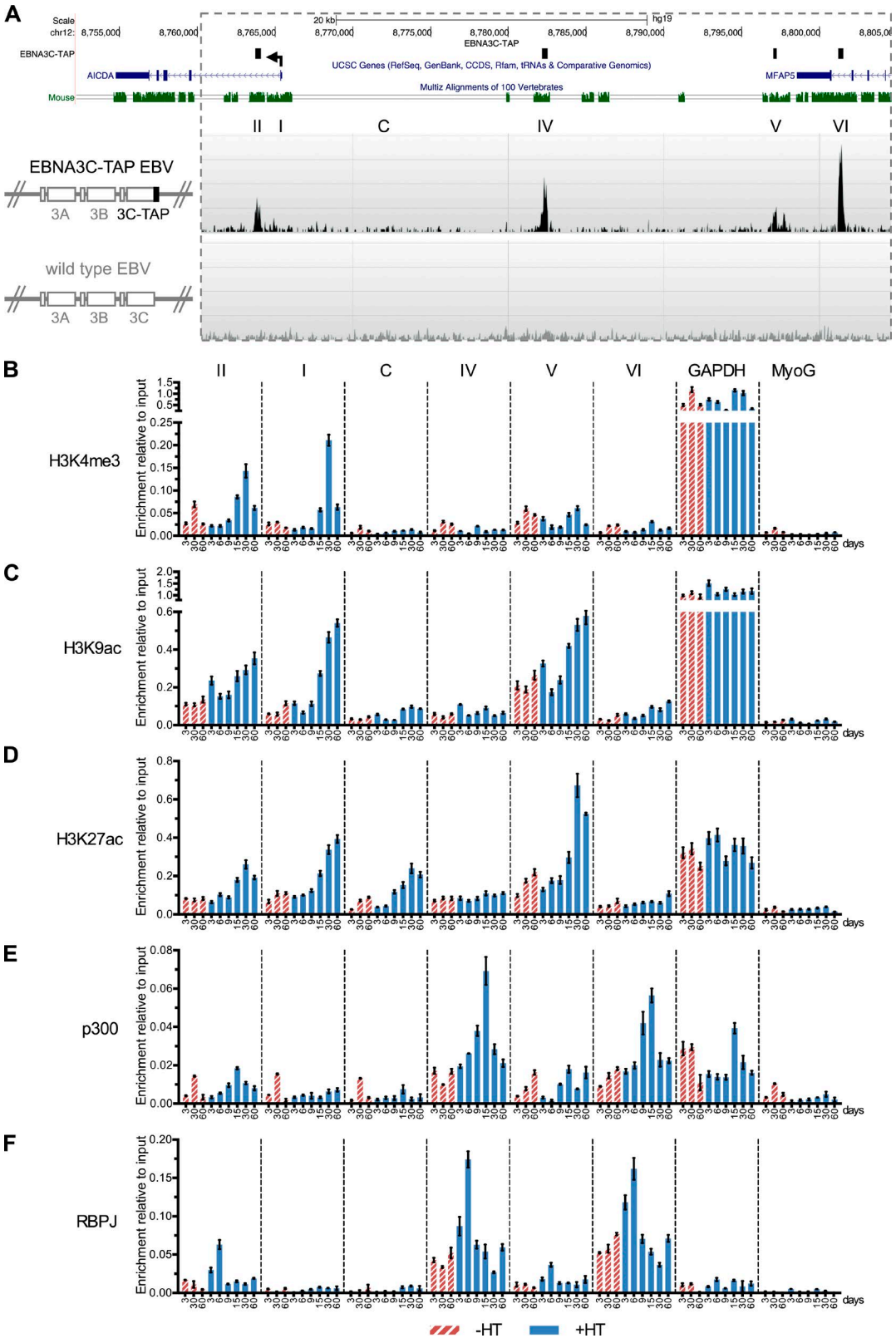

Figure 3. **EBNA3C specifically targets regulatory elements and epigenetically controls AID expression.** (A) University of California, Santa Cruz (UCSC) genome browser overview of AID genomic locus (*AICDA*) showing model-based analysis of ChIP-Seq (MACS) peaks for EBNA3C-TAP, mouse sequence alignment, and primer locations for ChIP-qPCR. Anti-Flag ChIP-Seq signals from EBNA3C-TAP–tagged and untagged wild-type LCLs were displayed

tion-associated histone marks H3K4me3, H3K9ac, and H3K27ac. There was an increase of H3K4me3 at regions I and II only when EBNA3C was functional (Fig. 3 B). Furthermore, there was an increase of H3K9ac and H3K27ac at these two sites and also on region V, again only when EBNA3C was functional (Figs. 3, C and D). One of the few transcriptional coactivators with which EBNA3C has been reported to physically interact is the histone acetyltransferase p300 (Subramanian et al., 2002). ChIP for p300 showed that there was a transient recruitment of p300 mainly to regions IV and VI, again only when EBNA3C was functional (Fig. 3 E). The timing of the recruitment is consistent with the increase in histone acetylation at regions I, II, and V; however, we were surprised because histone acetylation levels did not increase at regions IV and VI, the two sites where most p300 could be detected, but at sites up to 20 kb away from them. Consistent with this, it has been shown that in activated mouse B cells, regions IV, V, and VI form long-range interactions with regions I and II when AID is expressed (Kieffer-Kwon et al., 2013). This can also be seen in Hi-C data from GM12878 cells that express EBNA3C and relatively high levels of AID (Fig. 2 and Fig. S3; Rao et al., 2014). It is therefore likely that p300 binds at regions IV and VI but catalyzes the histone acetylation at regions I, II, and V. EBNA3C cannot bind directly to DNA, but recombination binding protein J (RBPJ; also known as CBF1/CSL), the Notch pathway–associated transcription factor, is a well characterized DNA-binding protein with which EBNA3C interacts (Allday et al., 2015), so ChIP for RBPJ was performed (Fig. 3 F). This revealed that RBPJ occupancy transiently increased at all regions where active EBNA3C was found, and the levels of recruited RBPJ correlated well with the levels of EBNA3C detected by ChIP-Seq (region VI > IV > II > V). Furthermore, the interaction between EBNA3C and RBPJ was shown to be essential for the induction of AID. Infection of primary B cells with recombinant EBV encoding an EBNA3C mutant for binding to RBPJ (Calderwood et al., 2011; Kalchschmidt et al., 2016) failed to induce AID expression (Fig. S1 B). Roles for RBPJ and p300 in the activation of Notch-regulated superenhancers have recently been described (Wang et al., 2014), so this is consistent with our observations of *AICDA* regulation by EBNA3C.

In summary, EBNA3C binds directly and specifically to four out of five of the well characterized regulatory elements of *AICDA*, probably in association with RBPJ and perhaps other transcription factors. Increased levels of activation-associated epigenetic marks are deposited, catalyzed at least in part by recruitment of p300, leading to active transcription.

EBNA3C via AID causes SHM at IgH V-D-J

To determine whether AID was functional after induction by EBNA3C in the 3CHT LCL, cDNA corresponding to the IgH V-D-J region from the 3CHT A13 LCL time course (Fig. 2 A) was subjected to deep DNA sequence analysis (Table S1). The clonal distribution within −HT and +HT samples was determined from the V-D-J recombined IgH sequences, which act as molecular barcodes for each B cell clone. The starting population of the time course contained four major clones that all exhibited productive V-D-J rearrangement and together comprised >90% of the culture (Fig. 4 A and Table S2). The clonal development over the 60-d time course was found to be similar between the −HT and +HT conditions and thus allowed us to directly compare the two (Fig. 4 A and Table S2). Sequence analysis revealed significantly more nucleotide changes in the V-D-J region of samples with functional EBNA3C (+HT) compared with nonfunctional EBNA3C (−HT) in all four analyzed major clones (Fig. 4 B). This was only detected from day 30 after activation of EBNA3C, which coincided with the time when the highest levels of AID were present (Fig. 2 A) and was further increased at day 60 in all four clones independently of whether the clone had undergone expansion or reduction in size (Fig. 4 B). These data are consistent with EBNA3C-activated AID being functional and inducing SHM at the IgH locus.

Summary and future perspective

We have shown that the EBV oncoprotein EBNA3C specifically targets highly conserved regulatory elements in *AICDA* and induces expression of AID in EBV-infected B cells. This then causes an increase in SHM at the IgH locus in non-GC B cells and might lead to genome-wide mutations. As a result, EBNA3C could potentiate the risk of EBV-infected B cells progressing to B cell malignancies. For ∼50 yr, it has been known that malaria and EBV infection in childhood are cofactors in eBL, but only recently was it shown that the parasite can directly induce AID expression and that chronic malaria infection creates GC environments favorable for the development of AID-dependent mature B cell lymphoma (Torgbor et al., 2014; Robbiani et al., 2015). Collectively with our data showing EBNA3C specifically targets and activates AID expression in EBV-infected B cells that could be the progenitors of BL, it is reasonable to speculate that the virus and parasite could synergize at this point in the etiology of eBL.

MATERIALS AND METHODS

Primary B cell infection. Recombinant EBNA3C KO and Rev viruses, virus production, and primary B cell isolation

in the Savant genome browser and are shown for the same genomic coordinates. (B–F) ChIP-qPCR for H3K4me3 (B), H3K9ac (C), H3K27ac (D), acetyltransferase p300 (E), and RBPJ (F) on samples from 3CHT A13 time course at locations across the AID locus at *GAPDH* or *myoglobin* as indicated. Cells were grown in the absence (−HT) or presence of HT (+HT), and numbers indicate the day of harvest. ChIP values represent enrichment relative to input ± SD of triplicate qPCR reactions for ChIP and input of each sample. These are representative results of two biological replicates.

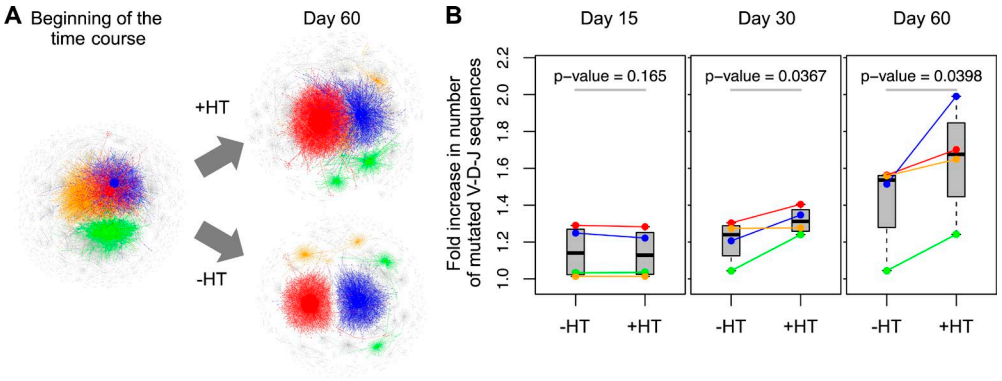

Figure 4. **EBNA3C via AID induces SHM at the IgH variable region.** (A) Network diagrams of B cell clones according to their rearranged V-D-J IgH sequence in samples of the 3CHT A13 time course show the clonal development of the four major clones (shown in red, blue, green, and orange) along minor clones (shown in gray) from the starting population at the beginning of the time course and after 60 d of culture with inactive (−HT) or active (+HT) EBNA3C. Each vertex represents a unique sequence, where relative vertex size is proportional to the number of identical reads. Edges join vertices that differ by single nucleotide differences, and clusters are collections of related, connected vertices. (B) Boxplots of the fold increase in the number of mutated V-D-J sequences for the four largest clones (same colors as in A) after 15, 30, and 60 d of culture with inactive (−HT) or active (+HT) EBNA3C. This is calculated as a cumulative change in the number of mutated V-D-J sequences at each time point relative to the starting population. P-values were determined by paired Student's *t* test.

have been described previously (Anderton et al., 2008; Skalska et al., 2013). B cell purity was assessed to be >90% $CD20^+$ using anti–CD20-APC (eBioscience) staining and flow cytometric analysis. RNA was harvested from uninfected primary B cells. Primary B cells (from anonymous donor buffy coats, purchased from the UK Blood Transfusion Service) were infected with virus-containing supernatant, and infected cells were incubated in RPMI 1640 (Thermo Fisher Scientific) supplemented with 15% fetal bovine serum, penicillin, and streptomycin at 37°C and 5% CO_2. Over a period of 30 d, infected cells were harvested for RNA extraction and replaced by fresh medium every 3 or 5 d.

Cell culture and time courses. All cells were cultured in RPMI 1640 medium supplemented with 10% fetal bovine serum, penicillin, and streptomycin either in the absence or presence of 400 nM HT (Sigma-Aldrich) at 37°C and 10% CO_2. For the time course experiments, EBNA3C-conditional LCLs (3CHT) on the p16-null background were used (Skalska et al., 2013). 3CHT A13 (established in the absence of HT) was used in a time course experiment over 60 d with RNA, protein, and ChIP samples taken every 3 d over the first 30 d and every 10 d until day 60. Cells were counted and diluted to 3×10^5 cells/ml at every time point until day 30 and three times a week subsequently, but seeded at 3×10^5 cells/ml the day before harvesting. After harvesting cells on day 30, the +HT culture was split in two, and for one of the cultures, the medium was replaced with fresh medium without HT, which was subsequently cultured without HT until day 60 (washed). Replicate 3CHT A13 and 3CHT C19 (established in the presence of HT, washed, and then grown without HT in the medium for >3 mo before the experiment was started) time courses were performed over a period of 60 d. Cells were counted and split to 3×10^5 cells/ml the day before harvesting samples for RNA, protein, and ChIP. The 3CHT C19 time course was also used as a biological replicate for the ChIP analysis and showed essentially the same results as the 3CHT A13 time course. To analyze the expression of AID across cell lines, three in-house B95.8 EBV–transformed LCLs, LCL GM12878, the EBV-negative BL cell line Ramos, the EBV-positive BL cell lines Akata, Oku, and Namalwa, the EBV-negative B cell lymphoma cell line BJAB, and the EBV-negative chronic myelogenous leukemia cell line K562 were cultured and split to 3×10^5 cells/ml the day before harvesting samples for RNA and protein.

RT-qPCR. RT-qPCR was performed essentially as described previously (Skalska et al., 2013). RNA from 4.5×10^6 cells was extracted using the RNeasy mini kit (QIAGEN), and 10 ng cDNA was used for each qPCR reaction. *GAPDH* or *GNB2L1* were used as housekeeping genes, and gene expression was expressed relative to primary B cells or LCL-HT on day 0 as indicated. The sequences of the primers used in this study are listed in Table S3.

Immunoblotting. Immunoblotting was performed essentially as described previously (Anderton et al., 2008; Skalska et al., 2013). A total amount of 30 µg of radioimmunoprecipitation assay protein extract was separated on 10% SDS-PAGE using a Mini-PROTEAN II cell (Bio-Rad Laboratories), transferred onto nitrocellulose membrane (Protran), and probed for AID (mAID-2; eBioscience) or γ-tubulin (T6557; Sigma-Aldrich).

ChIP. ChIPs for histone modifications, H3K4me3 (17-614; EMD Millipore), H3K9ac (17-658; EMD Millipore), and

H3K27ac (05-1334; EMD Millipore), were performed as described previously (Skalska et al., 2013). For anti-Flag (2368S; Cell Signaling Technology), p300-C20 (SC585X; Santa Cruz Biotechnology, Inc.), and RBPJ (ab25949; Abcam) ChIPs, 4.5 × 10^6 cells were incubated for 20 min in 1 ml of swelling buffer (25 mM Hepes, pH 7.8, 1.5 mM $MgCl_2$, 10 mM KCl, 0.1% NP-40, 1 mM DTT, 1 mM PMSF, 1 µg/ml aprotinin, and 1 µg/ml pepstatin A). Nuclei were resuspended in 1 ml of sonication buffer (50 mM Hepes, pH 7.8, 140 mM NaCl, 1 mM EDTA, 1% Triton X-100, 0.1% sodium deoxycholate, 0.1% SDS, 1 mM PMSF, 1 µg/ml aprotinin, and 1 µg/ml pepstatin A) and sonicated for 1 h using an M220 (75-W peak power and 26 duty cycle for 200 cycles/burst at 6°C set temperature; Covaris). Thereafter, a ChIP assay kit (17-295; EMD Millipore) was used according to the manufacturer's protocol. DNA was cleaned using a PCR purification kit (QIAquick; QIAGEN) and was assayed by qPCR on QuantStudio 7 Flex (Thermo Fisher Scientific). Input DNA was 5% of DNA used in immunoprecipitations and diluted to 2.5% before PCR quantification. Enrichment relative to input was calculated using four fivefold dilution series, and error bars were calculated as SDs from triplicate PCR reactions for both input and ChIP. Sequences of the primers used in these assays are listed in Table S4.

SHM analysis at the IgH V-D-J locus. Sequencing of the rearranged IgH V-D-J locus was performed as described previously (Bashford-Rogers et al., 2013). In brief, mRNA extracted from samples of the 3CHT A13 time course (see the Cell culture and time courses section) was reverse transcribed into cDNA that was used to PCR amplify IgH V-D-J as previously described. MiSeq libraries were prepared using Illumina protocols and sequenced using 300-bp paired-end MiSeq (Illumina). Raw MiSeq reads were filtered for base quality (median >32) using the QUASR program (Watson et al., 2013). Nonimmunoglobulin sequences were removed, and only reads with significant similarity to reference IgHV genes from the International Immunogenetics Information System database (Lefranc et al., 2009) using BLAST (Altschul et al., 1990) were retained (10^{-10} E-value threshold). Primer sequences were trimmed from the reads, and sequences were retained for analysis only if both primer sequences were identified. Network analyses were performed as described previously (Bashford-Rogers et al., 2013). To determine the fold increase in the number of mutated sequences in the top four clusters, the sequences from the HT+/− samples on days 0, 15, 30, and 60 were combined clustered according to the criteria in this paragraph. The largest four clusters in the combined dataset were identified, and the time point at which each unique B cell receptor was first observed was determined. On this basis, the fold increase in the number of mutated sequences was determined compared with the number of mutated sequences in each clone in the day 0 sample. P-values were determined by paired Student's *t* tests in R.

Online supplemental material. Fig. S1 shows that repression of BCL6 is independent of EBNA3C and that induction of AID is dependent on the ability of EBNA3C to interact with RBPJ. Fig. S2 shows ChIP-qPCR verification of EBNA3C occupancy at regulatory regions of *AICDA*. Fig. S3 shows the higher order chromatin structure of the *AICDA* locus in LCL GM12878. Table S1 provides additional information on the number of sequencing reads and unique V-D-J rearrangements per sample. Table S2 provides additional information on the four major clones analyzed. Table S3 lists primers used in RT-qPCR. Table S4 lists primers used in ChIP-qPCR. Online supplemental material is available at http://www.jem.org/cgi/content/full/jem.20160120/DC1.

ACKNOWLEDGMENTS

Funding was provided by the Wellcome Trust through a Senior Investigator award to M.J. Allday (099273/Z/12/Z) and a studentship to J.S. Kalchschmidt (097005).

The authors declare no competing financial interests.

Submitted: 25 January 2016

Accepted: 12 April 2016

REFERENCES

Allday, M.J. 2009. How does Epstein-Barr virus (EBV) complement the activation of Myc in the pathogenesis of Burkitt's lymphoma? *Semin. Cancer Biol.* 19:366–376. http://dx.doi.org/10.1016/j.semcancer.2009.07.007

Allday, M.J., Q. Bazot, and R.E. White. 2015. The EBNA3 family: two oncoproteins and a tumour suppressor that are central to the biology of EBV in B cells. *Curr. Top. Microbiol. Immunol.* 391:61–117. http://dx.doi.org/10.1007/978-3-319-22834-1_3

Altschul, S.F., W. Gish, W. Miller, E.W. Myers, and D.J. Lipman. 1990. Basic local alignment search tool. *J. Mol. Biol.* 215:403–410. http://dx.doi.org/10.1016/S0022-2836(05)80360-2

Anderton, E., J. Yee, P. Smith, T. Crook, R.E. White, and M.J. Allday. 2008. Two Epstein-Barr virus (EBV) oncoproteins cooperate to repress expression of the proapoptotic tumour-suppressor Bim: clues to the pathogenesis of Burkitt's lymphoma. *Oncogene.* 27:421–433. http://dx.doi.org/10.1038/sj.onc.1210668

Bashford-Rogers, R.J.M., A.L. Palser, B.J. Huntly, R. Rance, G.S. Vassiliou, G.A. Follows, and P. Kellam. 2013. Network properties derived from deep sequencing of human B-cell receptor repertoires delineate B-cell populations. *Genome Res.* 23:1874–1884. http://dx.doi.org/10.1101/gr.154815.113

Calderwood, M.A., S. Lee, A.M. Holthaus, S.C. Blacklow, E. Kieff, and E. Johannsen. 2011. Epstein-Barr virus nuclear protein 3C binds to the N-terminal (NTD) and beta trefoil domains (BTD) of RBP/CSL; only the NTD interaction is essential for lymphoblastoid cell growth. *Virology.* 414:19–25. http://dx.doi.org/10.1016/j.virol.2011.02.018

Epeldegui, M., Y.P. Hung, A. McQuay, R.F. Ambinder, and O. Martínez-Maza. 2007. Infection of human B cells with Epstein-Barr virus results in the expression of somatic hypermutation-inducing molecules and in the accrual of oncogene mutations. *Mol. Immunol.* 44:934–942. http://dx.doi.org/10.1016/j.molimm.2006.03.018

Gil, Y., S. Levy-Nabot, M. Steinitz, and R. Laskov. 2007. Somatic mutations and activation-induced cytidine deaminase (AID) expression in established rheumatoid factor-producing lymphoblastoid cell line. *Mol. Immunol.* 44:494–505. http://dx.doi.org/10.1016/j.molimm.2006.02.012

He, B., N. Raab-Traub, P. Casali, and A. Cerutti. 2003. EBV-encoded latent membrane protein 1 cooperates with BAFF/BLyS and APRIL to induce T cell-independent Ig heavy chain class switching. *J. Immunol.* 171:5215–5224. http://dx.doi.org/10.4049/jimmunol.171.10.5215

Heath, E., N. Begue-Pastor, S. Chaganti, D. Croom-Carter, C. Shannon-Lowe, D. Kube, R. Feederle, H.-J. Delecluse, A.B. Rickinson, and A.I. Bell. 2012. Epstein-Barr virus infection of naïve B cells in vitro frequently selects clones with mutated immunoglobulin genotypes: implications for virus biology. *PLoS Pathog.* 8:e1002697. http://dx.doi.org/10.1371/journal.ppat.1002697

Hwang, J.K., F.W. Alt, and L.-S. Yeap. 2015. Related mechanisms of antibody somatic hypermutation and class switch recombination. *Microbiol. Spectr.* 3:MDNA3-0037-2014. http://dx.doi.org/10.1128/microbiolspec.MDNA3-0037-2014

Kalchschmidt, J.S., A.C.T. Gillman, K. Paschos, Q. Bazot, B. Kempkes, and M.J. Allday. 2016. EBNA3C directs recruitment of RBPJ (CBF1) to chromatin during the process of gene repression in EBV infected B cells. *PLoS Pathog.* 12:e1005383. http://dx.doi.org/10.1371/journal.ppat.1005383

Kieffer-Kwon, K.-R., Z. Tang, E. Mathe, J. Qian, M.-H. Sung, G. Li, W. Resch, S. Baek, N. Pruett, L. Grøntved, et al. 2013. Interactome maps of mouse gene regulatory domains reveal basic principles of transcriptional regulation. *Cell.* 155:1507–1520. http://dx.doi.org/10.1016/j.cell.2013.11.039

Lefranc, M.-P., V. Giudicelli, C. Ginestoux, J. Jabado-Michaloud, G. Folch, F. Bellahcene, Y. Wu, E. Gemrot, X. Brochet, J. Lane, et al. 2009. IMGT, the international ImMunoGeneTics information system. *Nucleic Acids Res.* 37:D1006–D1012. http://dx.doi.org/10.1093/nar/gkn838

Qian, J., Q. Wang, M. Dose, N. Pruett, K.-R. Kieffer-Kwon, W. Resch, G. Liang, Z. Tang, E. Mathé, C. Benner, et al. 2014. B cell super-enhancers and regulatory clusters recruit AID tumorigenic activity. *Cell.* 159:1524–1537. http://dx.doi.org/10.1016/j.cell.2014.11.013

Rao, S.S.P., M.H. Huntley, N.C. Durand, E.K. Stamenova, I.D. Bochkov, J.T. Robinson, A.L. Sanborn, I. Machol, A.D. Omer, E.S. Lander, and E.L. Aiden. 2014. A 3D map of the human genome at kilobase resolution reveals principles of chromatin looping. *Cell.* 159:1665–1680. http://dx.doi.org/10.1016/j.cell.2014.11.021

Robbiani, D.F., and M.C. Nussenzweig. 2013. Chromosome translocation, B cell lymphoma, and activation-induced cytidine deaminase. *Annu. Rev. Pathol.* 8:79–103. http://dx.doi.org/10.1146/annurev-pathol-020712-164004

Robbiani, D.F., S. Deroubaix, N. Feldhahn, T.Y. Oliveira, E. Callen, Q. Wang, M. Jankovic, I.T. Silva, P.C. Rommel, D. Bosque, et al. 2015. Plasmodium infection promotes genomic instability and AID-dependent B cell lymphoma. *Cell.* 162:727–737. http://dx.doi.org/10.1016/j.cell.2015.07.019

Rowe, M., G.L. Kelly, A.I. Bell, and A.B. Rickinson. 2009. Burkitt's lymphoma: the Rosetta Stone deciphering Epstein-Barr virus biology. *Semin. Cancer Biol.* 19:377–388. http://dx.doi.org/10.1016/j.semcancer.2009.07.004

Schmitz, R., M. Ceribelli, S. Pittaluga, G. Wright, and L.M. Staudt. 2014. Oncogenic mechanisms in Burkitt lymphoma. *Cold Spring Harb. Perspect. Med.* 4:a014282. http://dx.doi.org/10.1101/cshperspect.a014282

Skalska, L., R.E. White, G.A. Parker, E. Turro, A.J. Sinclair, K. Paschos, and M.J. Allday. 2013. Induction of $p16^{INK4a}$ is the major barrier to proliferation when Epstein-Barr virus (EBV) transforms primary B cells into lymphoblastoid cell lines. *PLoS Pathog.* 9:e1003187. http://dx.doi.org/10.1371/journal.ppat.1003187

Skalsky, R.L., and B.R. Cullen. 2015. EBV noncoding RNAs. *Curr. Top. Microbiol. Immunol.* 391:181–217. http://dx.doi.org/10.1007/978-3-319-22834-1_6

Subramanian, C., S. Hasan, M. Rowe, M. Hottiger, R. Orre, and E.S. Robertson. 2002. Epstein-Barr virus nuclear antigen 3C and prothymosin alpha interact with the p300 transcriptional coactivator at the CH1 and CH3/HAT domains and cooperate in regulation of transcription and histone acetylation. *J. Virol.* 76:4699–4708. http://dx.doi.org/10.1128/JVI.76.10.4699-4708.2002

Thorley-Lawson, D.A. 2015. EBV persistence—introducing the virus. *Curr. Top. Microbiol. Immunol.* 390:151–209. http://dx.doi.org/10.1007/978-3-319-22822-8_8

Thorley-Lawson, D.A., and M.J. Allday. 2008. The curious case of the tumour virus: 50 years of Burkitt's lymphoma. *Nat. Rev. Microbiol.* 6:913–924. http://dx.doi.org/10.1038/nrmicro2015

Tobollik, S., L. Meyer, M. Buettner, S. Klemmer, B. Kempkes, E. Kremmer, G. Niedobitek, and B. Jungnickel. 2006. Epstein-Barr virus nuclear antigen 2 inhibits AID expression during EBV-driven B-cell growth. *Blood.* 108:3859–3864. http://dx.doi.org/10.1182/blood-2006-05-021303

Torgbor, C., P. Awuah, K. Deitsch, P. Kalantari, K.A. Duca, and D.A. Thorley-Lawson. 2014. A multifactorial role for *P. falciparum* malaria in endemic Burkitt's lymphoma pathogenesis. *PLoS Pathog.* 10:e1004170. http://dx.doi.org/10.1371/journal.ppat.1004170

Wang, H., C. Zang, L. Taing, K.L. Arnett, Y.J. Wong, W.S. Pear, S.C. Blacklow, X.S. Liu, and J.C. Aster. 2014. NOTCH1-RBPJ complexes drive target gene expression through dynamic interactions with superenhancers. *Proc. Natl. Acad. Sci. USA.* 111:705–710. http://dx.doi.org/10.1073/pnas.1315023111

Watson, S.J., M.R.A. Welkers, D.P. Depledge, E. Coulter, J.M. Breuer, M.D. de Jong, and P. Kellam. 2013. Viral population analysis and minority-variant detection using short read next-generation sequencing. *Philos. Trans. R. Soc. Lond. B Biol. Sci.* 368:20120205. http://dx.doi.org/10.1098/rstb.2012.0205

Young, L.S., and A.B. Rickinson. 2004. Epstein-Barr virus: 40 years on. *Nat. Rev. Cancer.* 4:757–768. http://dx.doi.org/10.1038/nrc1452

Zan, H., and P. Casali. 2013. Regulation of *Aicda* expression and AID activity. *Autoimmunity.* 46:83–101. http://dx.doi.org/10.3109/08916934.2012.749244